Intermediate Mass Fragment Emission Pattern in Peripheral Heavy-Ion Collisions at Fermi Energies

S. Piantelli, L. Bidini, G. Poggi, M. Bini, G. Casini, P. R. Maurenzig, A. Olmi, G. Pasquali, A. A. Stefanini, and N. Taccetti

Istituto Nazionale di Fisica Nucleare and Università di Firenze, I-50125 Florence, Italy

(Received 11 May 2001; published 15 January 2002)

The emission pattern in the $v_{perp} - v_{par}$ plane of intermediate mass fragments with $Z = 3-7$ (IMF) has been studied in the collision $^{116}Sn + ^{93}Nb$ at 29.5A MeV as a function of the total kinetic energy loss of the reaction. This pattern shows that for peripheral reactions most IMF's are emitted at velocities intermediate between those of the projectile- and target-like products. Coulomb trajectory calculations show that these IMF's are produced in the interaction zone in a short time interval at the end of the target-projectile interaction.

DOI: 10.1103/PhysRevLett.88.052701 PACS numbers: 25.70.Pq, 25.70.Lm

In collisions of heavy ions in the *Fermi regime*, i.e., at bombarding energies of (30–50)A MeV, an intense emission of intermediate mass fragments (IMF) at midvelocity has been evidenced [1–7]. For noncentral collisions, where the binary character of the reaction is preserved, the velocity region between the projectile- and target-like fragments (PLF and TLF) presents an intensity of particles unexpected on the basis of the statistical emission from the hot, fully accelerated main fragments. This emission may be seen as a step in the evolution from the fast three-body processes found at lower energies [8,9] to the fragmentation of the "participant zone" or the "fire-ball" at much higher energies. At the present time, the isospin composition of the midvelocity light charged particles ($Z \leq 2$, LCP) and IMF's is highly debated, as it can be connected with the composition of the emitting source (see, e.g., [10] and references therein). The question of the mechanism responsible for these midvelocity emissions is also under discussion, due to the fact that for their interpretation both dynamical [6] and statistical approaches [11] have been used.

It was shown by the INDRA Collaboration [7] that, for a given bombarding energy, the largest ratio (up to ≈ 3) of *midvelocity* to *evaporative* IMF's is found in noncentral collisions. However, because of the relatively high threshold for TLF detection of the existing 4π detectors, so far it has not been possible to reliably select the very peripheral collisions. In this Letter we present experimental results which, thanks to the low thresholds for TLF detection, make it possible — for the first time — to identify reactions where almost all IMF's concentrate at midvelocity and to carefully study their emission pattern. Preliminary results were presented in Ref. [10].

The experiment (Florentine Initiative After Superconducting Cyclotron Opening, FIASCO) was performed at the Laboratori Nazionali del Sud in Catania (Italy). Targets of ^{93}Nb ($\approx 200\ \mu g/cm^2$) were bombarded with a 29.5A MeV pulsed beam of ^{116}Sn, with intensity ≤ 0.1 nA and time resolution ≤ 1 ns. The setup basically consisted of 24 position-sensitive parallel plate avalanche detectors (PPAD) [12,13] covering $\approx 70\%$ of the forward solid angle, down to a minimum angle of 0.8°. They measured, with very low thresholds ($< 0.1A$ MeV), impact time and position (FWHM resolutions 600 ps and 3.5 mm, respectively) of heavy reaction products ($A \geq 20$). From the velocity vectors, primary (i.e., preevaporative) quantities (including the total kinetic energy loss, TKEL [12]) were kinematically reconstructed event by event [14]. The setup included 160 two- and three-element phoswich scintillators mounted behind most of the PPAD's. They detected LCP's and IMF's with $Z \leq 20$ in $\approx 20\%$ of the forward solid angle (plus a reduced sampling in the backward hemisphere). The first element of the phoswiches was a 200 μm thin fast-plastic scintillator resulting in rather low thresholds [$\approx (3-10)A$ MeV for $Z = 1-20$]. The measurement of the time of flight allowed us to directly obtain the velocities of LCP's and IMF's, without tricky and time-consuming energy calibrations of the scintillators. A detailed description of the setup was given in [15].

The data presented in this Letter are focused on binary events, where only two major fragments are detected in the PPAD's while the coincident LCP's and IMF's hit the phoswich detectors. Using TKEL as an ordering variable, one can select events with increasing impact parameters up to grazing collisions. Contrary to all other available 4π detectors, our low thresholds also allow us to measure both the PLF and the TLF for events with TKEL ≤ 400 MeV. Reconstructed primary quantities were obtained from two-body kinematics for events with emission not only of LCP's, but also of an IMF [16].

The left part of Fig. 1 shows, for TKEL = 240–400 MeV, the experimental yields of p, d, He, and IMF's ($Z = 3-7$) in the $v_{perp}-v_{par}$ plane. Here v_{par} and v_{perp} are, respectively, the velocity components parallel and perpendicular to the asymptotic PLF-TLF axis in the target-projectile center of mass system (differing by only 4 mm/ns from the nucleon-nucleon one, due to the small

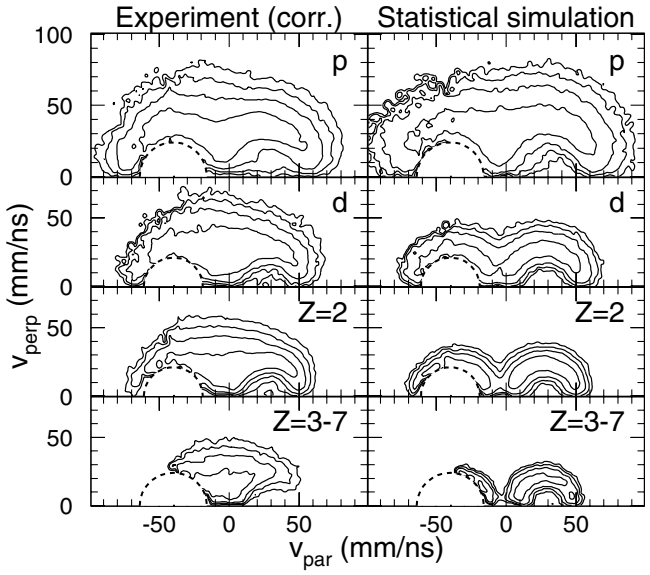

FIG. 1. Left: experimental yields in the v_{perp}-v_{par} plane for p, d, He, and IMF's ($Z = 3-7$) in the system ^{116}Sn + ^{93}Nb at 29.5A MeV, for TKEL = 240−400 MeV (corrected for the setup geometry). Level spacing is logarithmic, dashed lines indicate velocity thresholds. Right: same results for the simulated evaporative emission from the hot reaction partners.

asymmetry of the entrance channel). Dashed lines show the velocity thresholds due to the thin fast-plastic scintillator. The data were corrected with Monte Carlo methods for the efficiency and finite geometry of the setup [15]; because of its large acceptance and axial symmetry, the correction is largely independent of the emission pattern. In the backward lab hemisphere ($v_{par} \lesssim -40$ mm/ns), due to the reduced detector coverage, the correction is not as effective as in the forward one.

In order to better clarify the major features of the experimental data, the right-hand panels of Fig. 1 show the corresponding yields obtained with the simulation of a pure evaporation from fully accelerated fragments, filtered with the setup acceptance and then corrected in the same way as the experimental data. The excitation energy of the fragments was obtained from TKEL with an "equal energy" sharing, according to [17]. For the evaporation step, the statistical code GEMINI [18] was used, but the LCP and IMF multiplicities had to be adjusted to reproduce the experimental ones.

The experimental emission pattern for protons does not differ very much from that expected for a sequential evaporation, but with increasing particle mass the midvelocity yield becomes increasingly important until it actually exhausts most of the IMF intensity.

The midvelocity particle multiplicities were obtained with a procedure similar to that outlined in [6]. The simulation of the evaporation step was tuned so as to reproduce the experimental data in the velocity region corresponding to forward emission from the PLF ($10° \leq \theta_{PLF} \leq 40°$ in the PLF reference frame). Assuming that it properly mimics the whole evaporative emission of PLF and TLF, the midvelocity yield is obtained as the difference between the total experimental emission and the corresponding estimate of the evaporative component.

The deduced multiplicities are shown as a function of TKEL in Fig. 2, separately for p, d, t, He, and IMF's. Full circles refer to the statistical evaporation, with uncertainties (due to detector thresholds and determination of the TLF emission) usually smaller than the symbol size. Full squares show the multiplicity of midvelocity particles. The larger the midvelocity component, the more reliable its extraction; the largest errors are for protons, owing to the presence of a large evaporative component.

It is worth noting that in the midvelocity emission of peripheral events, the mass removed by the IMF's

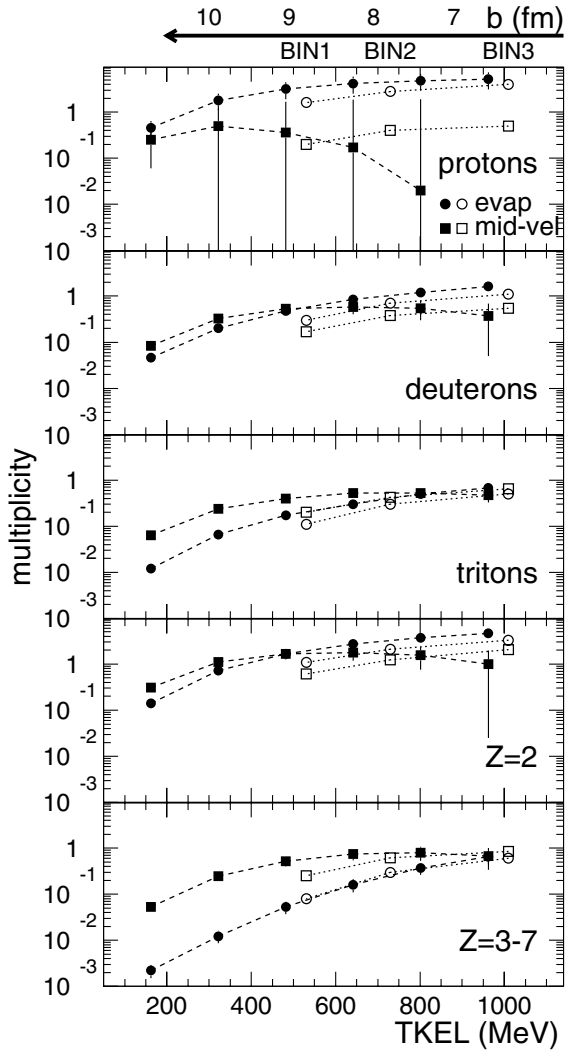

FIG. 2. Experimental multiplicities of p, d, t, He, and IMF's ($Z = 3-7$) against TKEL in ^{116}Sn + ^{93}Nb at 29.5A MeV. Full squares (circles) refer to the midvelocity (evaporative) component; open symbols are for the system Xe + Sn at 32A MeV [7]. Lines are to guide the eye. On top, correspondence between TKEL and impact parameter (or centrality binning of [7]), estimated from the QMD code CHIMERA [19].

(assuming $A \approx 2Z$) is comparable to that removed by LCP's (while it is much smaller in case of evaporation). Moreover, as already qualitatively seen in Fig. 1, the midvelocity component of IMF's greatly overcomes the evaporative emission by more than a factor of 20 for the most peripheral collisions. To our knowledge, this extremely enhanced emission of midvelocity IMF's has never been directly observed before; the nuclear matter tends to break apart in intermediate mass fragments, and this process successfully competes with LCP emission.

The comparison of the multiplicities presented in Fig. 2 with those of Xe + Sn (open symbols) at similar bombarding energies [7] required us to find a correspondence between our ordering variable (TKEL) and that used by the INDRA Collaboration to estimate the impact parameter (transverse energy of LCP's, E_{trans12}). Following Ref. [7], we used the same quantum molecular dynamics (QMD) code CHIMERA [19] as an event generator for our reaction ^{116}Sn + ^{93}Nb. In simulated events, analyzed in the same way as the experimental ones, the reconstructed TKEL is closely correlated with the impact parameter [20]; details are given in [15]. Here, on top of Fig. 2, we have synthetically drawn the obtained impact parameter scale. It has to be noted that the range of impact parameters probed by our experiment extends to significantly larger values than those accessible with INDRA, the results of both experiments being in good agreement in the common region.

To deal with the question of whether the production mechanism of midvelocity IMF's is mainly of a dynamical or statistical nature is beyond the scope of this Letter, but the peculiar emission pattern of the very peripheral collisions (where it is almost free from contaminations due to evaporation from PLF and TLF) can give information on the time-space configuration of the emitting system.

First of all, an emission from PLF and TLF alone would not produce the large yield of midvelocity IMF's with large transverse momenta. In fact, even in the case of a fast nonequilibrium process, the IMF's would still be pushed (possibly in an anisotropic way) on portions of Coulomb rings. Therefore a midvelocity emission was assumed, the IMF being the remnant of the overlapping nuclear matter ("neck" or "participant zone"). Schematically, the Coulomb trajectory calculation was performed by numerical integration of the three-body classical equations of motion starting from the following initial conditions: (1) The three objects are in an aligned configuration, at the end of the interaction phase. Distances d_{sep} between the PLF and TLF surfaces in the range 5–12 fm were considered, the lower value corresponding to three touching spheres and the upper one to a very elongated neck [21]. At the considered relative velocities, this upper limit corresponds to times of $\approx$60 fm/c. Since the results are not very sensitive to its specific value, d_{sep} was randomly varied in the mentioned range. (2) Positions and velocities of PLF and TLF are obtained by analytically bringing back these two fragments (produced by a realistic two-body Monte Carlo simulation) on their Coulomb trajectories until their surfaces are at the distance d_{sep} (the correspondence between TKEL and impact parameter was deduced from the QMD code). (3) The IMF, sampled from a charge distribution deduced from the experimental data, is emitted halfway between PLF and TLF with a mean velocity intermediate between those of PLF and TLF (nucleon-nucleon system) plus a random "thermal-like" kinetic energy described by a tuning parameter $\langle E_n \rangle$.

Figure 3a presents the emission pattern obtained after applying the experimental filter, in the bin TKEL = 240–400 MeV (with $\langle E_n \rangle = 25$ MeV). The main effect of the two close-lying fragments is to partly deplete the high values of v_{par}, while the shape of the v_{perp} distribution mainly depends on the assumed thermal-like energy. In fact, for peripheral collisions, the heavy fragments fly swiftly apart, with little energy transfer to the IMF. The comparison with the experimental correlation (Fig. 3d) shows that the simulated *midvelocity emission* significantly contributes to the experimental distribution, in particular in the high transverse momentum region, but is too narrow in the parallel momentum. This can be better seen in Figs. 3e–3f where the experimental v_{par} and v_{perp} distributions (full dots) are compared to the simulated ones (dashed histograms).

Further simulations with different modeling of the IMF emission have shown the following: (a) variations of its spatial position (up to a flat distribution across the whole gap between the two main fragments) do not appreciably alter the emission pattern; (b) variations of its initial mean

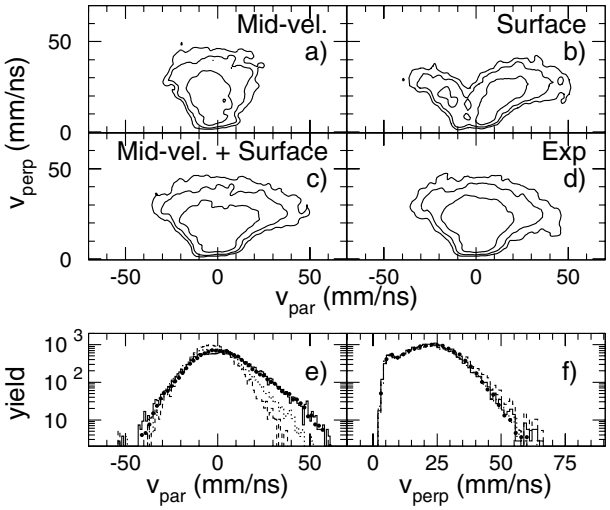

FIG. 3. Plots of v_{perp}-v_{par} for IMF's ($Z = 3$–7) at TKEL = 240–400 MeV: (a) Coulomb trajectory calculation for *midvelocity emission* with $\langle E_n \rangle = 25$ MeV and (b) for *surface emission* with $\langle E_s \rangle = 10$ MeV, (c) mixture of the two, and (d) experimental correlation. Projection on (e) v_{par} and (f) v_{perp} of the experimental (full dots) and simulated yields [histograms: dashed for the correlation in (a); dotted for an extended source, see text; continuous for the correlation in (c)].

velocity (with respect to that of the nucleon-nucleon system) have little effect unless values close to that of PLF or TLF are considered. The dotted histograms of Figs. 3e–3f show the result of a simulation where the initial spatial position of the IMF is evenly distributed across the gap between PLF and TLF and its initial mean velocity correspondingly spans the whole range between PLF and TLF velocities. The disagreement with the experiment has been considerably reduced. This suggests that further improvement might be obtained by assuming that an even larger amount of IMF's are emitted nearly at rest in the PLF or TLF reference frame, from a quasialigned configuration somewhat reminiscent of the so-called "fast oriented fission" [8,13] or "aligned breakup" [9].

In order to keep the schematization simple (and the number of parameters small), we preferred to add to the central emission of Fig. 3a just a second component, namely a fast *surface emission*. It was assumed that the IMF's are emitted from the original contact regions on the surfaces of the two flying-apart primary fragments, with the velocity of PLF or TLF and, superimposed, a "thermal-like" energy $\langle E_s \rangle$. The overall agreement could be significantly improved only by allowing some spread of the emission point on the surface of the nuclei, which may be justified by shape fluctuations and/or angular momentum effects. Figure 3b shows the emission pattern of this surface emission (for $\langle E_s \rangle = 10$ MeV and a two-dimensional Gaussian spread around the contact point with $\sigma_\theta \approx 40°$): the resulting incomplete Coulomb rings reproduce the wings of the experimental distribution. A combination of the two components can now give a satisfactory reproduction of the experimental data, as shown in Fig. 3c, where a ratio between surface and midvelocity emission of 0.7 has been used. The projections of the experimental and simulated data (full dots and continuous histograms, respectively) on v_{par} (Fig. 3e) and v_{perp} (Fig. 3f) give us a better perception of the good quality of the agreement obtained. Thus a single mechanism aiming at a good reproduction of the experimental pattern should be modeled in such a way as to include, besides a central emission, also an important emission from phase space regions very near to those of the PLF and TLF. An agreement of the same quality is found for more peripheral events (TKEL $\leq$ 240 MeV), while for more central TKEL bins the comparison becomes increasingly blurred by the growing contribution of the evaporative emission. The overall trend is that both the random energy $\langle E_n \rangle$ of the midvelocity emission and the spread of the emission point in the surface emission increase with increasing centrality. Thus, in the proposed approach, the experimental IMF emission appears to be compatible with the formation of an extended neck-like structure which decays by a prompt emission from the neck region itself or induces a successive emission from the surfaces of the separating nuclei. In this framework, the midvelocity emission develops on a time scale of the order of the contact time of the two colliding nuclei, while for the surface emission a somewhat longer time extension is estimated. In fact, from the observed angular anisotropy and using realistic values of the angular momenta ($L \approx 30\hbar$) and moments of inertia of the nuclei (rigid sphere), one can exclude times significantly larger than about 300 fm/c. This value is of the order of that estimated in [8] for the most asymmetric fission-like processes.

In conclusion, peripheral collisions are characterized by a sizable emission of IMF's at midvelocity, successfully competing with LCP's and greatly overcoming the IMF evaporative emission. The peculiar pattern of midvelocity IMF's from peripheral collisions seems to require the emission from an "extended neck," which also includes a fast contribution of IMF's emitted nearly at rest in the PLF or TLF reference frame.

We thank J. Łukasik for providing us with the QMD code CHIMERA, R. Ciaranfi and M. Montecchi for developing dedicated electronics, and P. Del Carmine for help in the setup preparation. Many thanks are due to L. Calabretta and the machine crew of the LNS for their continuous efforts to provide a good quality pulsed beam.

[1] D. R. Bowman *et al.,* Phys. Rev. Lett. **70**, 3534 (1993).
[2] C. P. Montoya *et al.,* Phys. Rev. Lett. **73**, 3070 (1994).
[3] J. Tõke *et al.,* Phys. Rev. Lett. **75**, 2920 (1995).
[4] J. F. Dempsey *et al.,* Phys. Rev. C **54**, 1710 (1996).
[5] J. Tõke *et al.,* Phys. Rev. Lett. **77**, 3514 (1996).
[6] J. Łukasik *et al.,* Phys. Rev. C **55**, 1906 (1997).
[7] E. Plagnol *et al.,* Phys. Rev. C **61**, 014606 (2000).
[8] G. Casini *et al.,* Phys. Rev. Lett. **71**, 2567 (1993).
[9] F. Bocage *et al.,* Nucl. Phys. **A676**, 391 (2000).
[10] G. Poggi, Nucl. Phys. **A685**, 296c (2001).
[11] A. Botvina *et al.,* Phys. Rev. C **59**, 3444 (1999).
[12] R. J. Charity *et al.,* Z. Phys. A **341**, 53 (1991).
[13] A. A. Stefanini *et al.,* Z. Phys. A **351**, 167 (1995).
[14] G. Casini *et al.,* Nucl. Instrum. Methods Phys. Res., Sect. A **277**, 445 (1989).
[15] S. Piantelli Ph.D. thesis, Firenze, 2001.
[16] It was checked that in case of emission of just one IMF (the average IMF multiplicity is well below 1 for semiperipheral collisions) good agreement is found between the results of the analysis with the two-body kinematics (ignoring the IMF) and with the three-body kinematics (including the IMF as a third body).
[17] G. Casini *et al.,* Eur. Phys. J. A **9**, 491 (2000).
[18] R. J. Charity *et al.,* Nucl. Phys. **A483**, 371 (1988).
[19] J. Łukasik and Z. Majka, Acta Phys. Pol. B **24**, 1959 (1993).
[20] The same analysis showed that, because of the reduced acceptance of our setup, the E_{trans12} selection gave no narrow correlation with the impact parameter.
[21] U. Brosa and S. Grossmann, J. Phys. G **10**, 933 (1984).